Deep-Sea Research I 57 (2010) 1444–1453

Contents lists available at ScienceDirect

Deep-Sea Research I

journal homepage: www.elsevier.com/locate/dsri

Speciation of Fe in the Eastern North Atlantic Ocean

C.-E. Thuróczy [a,*], L.J.A. Gerringa [a], M.B. Klunder [a], R. Middag [a], P. Laan [a], K.R. Timmermans [a], H.J.W. de Baar [a,b]

[a] Royal Netherlands Institute for Sea Research (Royal NIOZ), P.O. BOX 59, 1790 AB Den Burg, Texel, The Netherlands
[b] Department Ocean Ecosystems, University of Groningen, The Netherlands

ARTICLE INFO

Article history:
Received 2 December 2009
Received in revised form
5 August 2010
Accepted 9 August 2010

Keywords:
Iron
Speciation
Complexation
Size fractionation
Ultra-filtration
Organic ligands
Particulate iron
Unfiltered
Colloids
Eastern North Atlantic
GEOTRACES

ABSTRACT

In the Eastern North Atlantic Ocean iron (Fe) speciation was investigated in three size fractions: the dissolvable from unfiltered samples, the dissolved fraction (<0.2 μm) and the fraction smaller than 1000 kDa (<1000 kDa). Fe concentrations were measured by flow injection analysis and the organic Fe complexation by voltammetry. In the research area the water column consisted of North Atlantic Central Water (NACW), below which Mediterranean Overflow Water (MOW) was found with the core between 800 and 1000 m depth. Below 2000 m depth the North Atlantic Deep Water (NADW) proper was recognised. Dissolved Fe and Fe in the <1000 kDa fraction showed a nutrient like profile, depleted at the surface, increasing until 500–1000 m depth below which the concentration remained constant. Fe in unfiltered samples clearly showed the MOW with high concentrations (4 nM) compared to the overlying NACW and the underlying NADW, with 0.9 nM and 2 nM Fe, respectively. By using excess ligand (Excess L) concentrations as parameter we show a potential to bind Fe. The surface mixed layer had the highest excess ligand concentrations in all size fractions due to phytoplankton uptake and possible ligand production. The ratio of Excess L over Fe proved to be a complementary tool in revealing the relative saturation state of the ligands with Fe. In the whole water column, the organic ligands in the larger colloidal fraction (between 0.2 μm and 1000 kDa) were saturated with Fe, whereas those in the smallest fraction (<1000 kDa) were not saturated with Fe, confirming that this fraction was the most reactive one and regulates dissolution and colloid aggregation and scavenging processes. This regulation was remarkably stable with depth since the alpha factor (product of Excess L and K'), expressing the reactivity of the ligands, did not vary and was 10^{13}. Whereas, in the NACW and the MOW, the ligands in the particulate (>0.2 μm) fraction were unsaturated with Fe with respect to the dissolved fraction, thus these waters had a scavenging potential.

1. Introduction

Dissolved iron (DFe) in seawater (<0.2 μm) consists of several size classes of colloidal Fe next to an operationally defined soluble pool ($<$ smallest size cut-off ultra-filtration; Nishioka et al., 2005). Organic Fe(III)-complexes exist within both the colloid pool(s) and the soluble pool (Boye et al., 2005) and are characterised by a very high conditional binding strength ($\log K' \approx 20$–23; Gledhill and van den Berg, 1994). These organic ligands bind Fe(III) so strongly that more than 99% of Fe in the oceans is in the organically complexed form (Rue and Bruland, 1997; Boye and van den Berg, 2000; Croot et al., 2001; Gerringa et al., 2006). Therefore ligands prevent Fe(III) from precipitating as oxyhydroxides and enable Fe to remain dissolved above concentrations determined by the solubility product (Kuma et al., 1996; Millero, 1998). In the ocean surface layer the speciation of Fe regulates its availability to phytoplankton and other micro-organisms, which also influence the Fe speciation: on the one hand Fe is consumed by these micro-organisms and on the other hand they can produce organic ligands (Rue and Bruland, 1997; Boye and van den Berg, 2000; Croot et al., 2001; Gerringa et al., 2006). In the deep ocean, organic complexation and the distribution over different size fractions determines precipitation and adsorption on particles. The quasi-equilibrium competition between dissolved organic complexation, colloid size class particles and fine suspended particles is deemed to control the removal by scavenging via settling of large particles and thus the deep ocean residence time of Fe (Fig. 1, made after de Baar and de Jong, 2001). According to Nishioka and Takeda (2000) and Nishioka et al. (2005) the small colloidal fraction (in their papers defined as between 200 kDa and 0.2 μm) is a very reactive fraction. Moreover Bergquist et al. (2007) concluded that variations in dissolved Fe are due to changes in the colloidal fraction (in their paper between 0.02 and 0.4 μm) in the Atlantic Ocean.

* Corresponding author. Tel.: +31 222 369 459.
E-mail address: Charles-Edouard.Thuroczy@nioz.nl (C.-E. Thuróczy).

0967-0637/$ - see front matter Crown Copyright © 2010 Published by Elsevier Ltd. All rights reserved.
doi:10.1016/j.dsr.2010.08.004

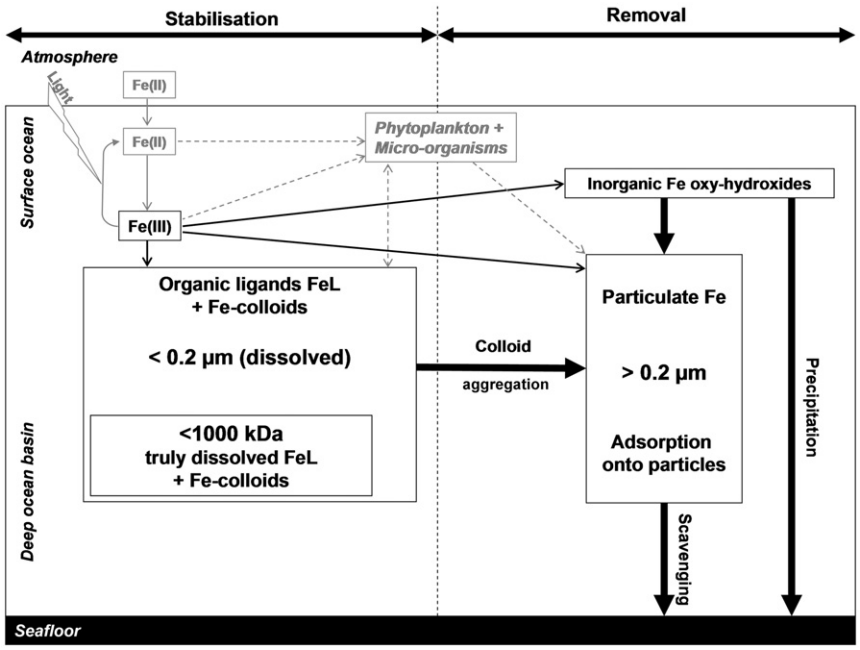

Fig. 1. Schematic representation of the Fe chemistry in the ocean. In the surface layer phytoplankton consumes Fe and produces organic ligands. Photo-reduction of Fe is indicated in grey since it is not considered in this paper. Organic ligands in the dissolved fraction (<0.2 µm) and within the smaller fraction (<1000 kDa) increase the residence time of Fe in the ocean by binding Fe, thus keeping the concentration of inorganic Fe low, preventing from precipitation as oxy-hydroxides, and restricting scavenging via adsorption onto particles. Finally, colloid aggregation is a possible pathway for removing Fe from the dissolved phase.

Here we investigate the processes of solubilisation through complexation versus scavenging and precipitation (Fig. 1) to gain insight into the cycling of Fe by sampling a deep profile at a station in the Eastern North Atlantic Ocean. Therefore we focus on size fractionation within the Fe-pool to study the organic complexation of Fe in three size fractions: the unfiltered samples (UNF), the dissolved fraction (<0.2 µm) and the fraction smaller than 1000 kDa.

2. Material and methods

2.1. Sampling and filtration

Samples were collected aboard R.V. Pelagia between April 11 and April 26, 2007, during the IPY-Geotraces (GEOTRACES Science Plan, 2006) cruise (64PE267) in the Eastern North Atlantic Ocean off the coast of Portugal (Fig. 2). Water samples were collected from station 14 (39°44′N–14°10′W), where six hydrocasts were performed for trace metals and nutrients (casts 1, 4, 5, 7, 18 and 20, Middag et al., submitted for publication). The first cast was sampled on April 19 for size fractionation and the measurements of organic speciation of Fe.

Analyses of Fe and the ligand characteristics were done on samples in three different size fractions:

1. Unfiltered samples (UNF), also called dissolvable fraction, containing the particulate fraction (>0.2 µm),
2. The dissolved fraction, defined as <0.2 µm,
3. The fraction smaller than 1000 kDa (<1000 kDa), containing the truly soluble and also the small colloidal fraction.

Fe in the unfiltered fraction is called Fe_{UNF}; Fe in the dissolved fraction is DFe and Fe in the fraction smaller than 1000 kDa is $Fe_{<1000\ kDa}$.

Samples were taken using 24 internally Teflon-coated PVC 12 l GO-FLO samplers (General Oceanics Inc.) mounted on the Titan Mk. II frame which was connected to a Kevlar hydrowire (de Baar et al., 2008). Immediately upon recovery the frame was placed inside a clean container for a direct sub-sampling from each GO-FLO sampler. First, the unfiltered samples were taken, after which the seawater left was filtered over a 0.2 µm pore size filter cartridge (Sartobran-300, Sartorius) under slight nitrogen gas overpressure. All sample bottles (used for storage of reagents and samples for trace metals) were Low Density Poly Ethylene bottles (LDPE, Nalgene) with volumes ranging from 60 ml (Fe analysis by FIA) to 1000 ml (Fe speciation), and were trace metal cleaned according to the procedure described in Middag et al. (2009).

Ultra-filtration of the 0.2 µm filtered water was performed in a clean room onboard, using hollow-fibre-filters (Sterapore, Mitsubishi-rayon Co., Ltd.) with a size cut-off of 1000 kDa (Nishioka et al., 2001) using a 12 channels (ISM 937, Ismatec, IPC-N) pump and Tygon® LFL (Long Flex Life) tubing. Before the cruise, the polyethylene hollow-fibre-filters were treated according to the following protocol (after Nishioka et al., 2001): They were activated by pumping 15 ml of three times quartz distilled (3QD)-methanol (flow rate of 5 ml min^{-1}), then rinsed with 30 ml MQ water. They were left soaking for 3 days in an HCl bath (1 M, Suprapur, Merck) during which each day 25 ml of HCl 1 M was pumped through the filter (5 ml min^{-1}). Then, they were rinsed with MQ water (140 ml, 7 ml min^{-1}) and stored in acid-cleaned polypropylene tubes closed by caps and filled with acidified MQ water (0.02 M HCl, Suprapur, Merck). Before use on board the ship the filters were rinsed by pumping MQ water (300 ml, 7 ml min^{-1}) and the sample itself (200 ml, 7 ml min^{-1}).

A mass balance was measured in 4 samples from the Southern Ocean. Two samples from the surface layer, containing 0.134 and 0.162 nM Fe, respectively, and two deep samples near the sediment containing 0.870 and 0.994 nM Fe, respectively, were used. The sum of the colloidal (here assumed to be between 1000 kDa and 0.2 µm) and <1000 kDa fractions was compared with the dissolved fraction (<0.2 µm). This resulted for the Excess L concentration in surface samples in a gain of Excess L concentration of 0.23 Eq of nM Fe and in the deep samples in a

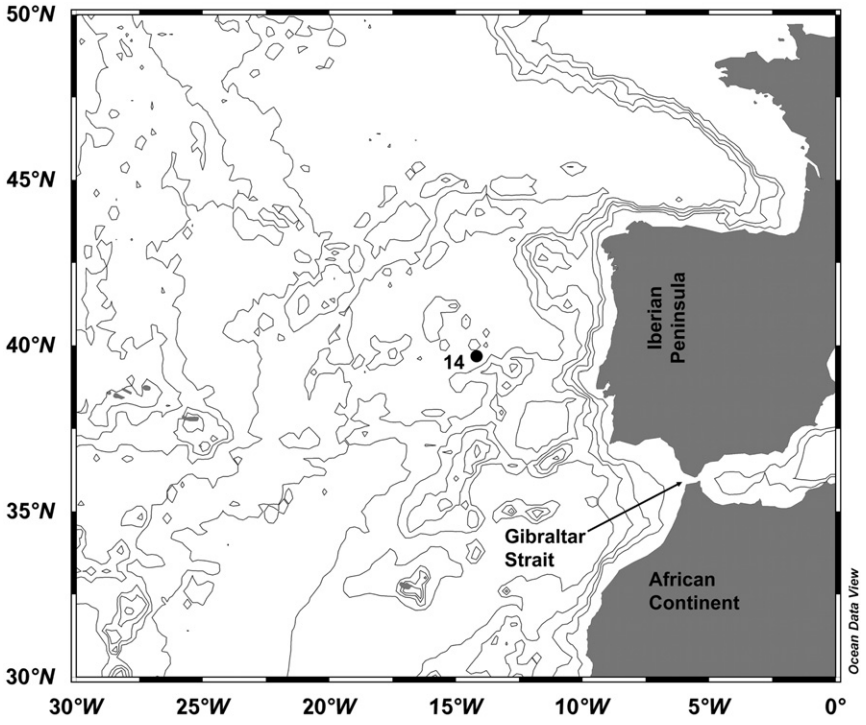

Fig. 2. Chart showing station 14 (39°44′N–14°10′W). The displayed isobaths are 1000, 2000, 3000, 4000 and 5000 m in depth.

loss of 0.05 Eq of nM Fe, whereas no Fe contamination was detected in the filtrate and in the retentate.

Iron analysis in unfiltered (Fe_{UNF}) samples and samples <1000 kDa was done from the same cast (Cast 1). Unfortunately, the results of DFe from this cast could not be used due to a contamination of the FIA chemiluminescence system by the buffer; therefore, the DFe concentrations from cast 18 (April 24) were used to calculate the speciation (see next).

To overcome problems with the interpretation of the results due to variations between casts in DFe over the period of sampling, speciation data was interpreted as "Excess L" concentrations ($[\text{Excess L}]_{\text{fraction}}=[\text{Lt}]_{\text{fraction}}-[\text{Fe}]_{\text{fraction}}$). Excess L represents the empty binding sites for Fe (concentration of empty ligand sites for Fe), thus a potential for binding Fe. The use of Excess L for interpretation of the organic complexation of Fe was also used by others (Rijkenberg et al., 2008a; Boye et al., 2001).

Nutrient, DFe, DMn and DAl data showed very little variation between the different casts (Middag et al., submitted for publication) indicating that water masses did not change in time. Indeed, standard deviations in DFe between casts 18 and 20 were very small (0.04 nM Fe on average).

Salinity (conductivity), temperature and depth (pressure) were measured with the CTD (Seabird SBE 911+) mounted on the titanium frame (de Baar et al., 2008).

2.2. Iron analyses

Iron analyses were done by an in-line flow injection analysis (FIA) system using chemiluminescence as a detection method (De Jong et al., 1998). This method was slightly modified, as described next. Samples were acidified to pH 1.8 using 12 M ultraclean HCl (Baseline® Hydrochloric Acid, Seastar Chemicals Inc.). The filtered samples (<0.2 μm and <1000 kDa fractions) were measured directly onboard and left acidified for at least 12 h before analysing. The unfiltered samples were acidified in the same way, but they were stored 1 year before being analysed in the home laboratory using the same system and procedure in a class 100 clean-room.

The method analyses Fe(III), therefore hydrogen peroxide (Merck suprapur 30%) solution was added (60 μl of a 1‰) at least 1 h before analysis to ensure oxidation of the Fe(II) present (Lohan et al., 2005). The acidified samples were preconcentrated over a Toyopearl AFChelate 650 M (TesoHaas Germany) column during 120 s. Subsequently the column was rinsed with MQ for 60 s, after which Fe was eluted with 0.4 M HCl (Suprapur, Merck) for 120 s and injected in the photon counter (Hamamatsu HC 135). The system was controlled by an interface developed in LabView. This method is described in more detail by Klunder et al. (in press). The standard deviation of the duplicate measurements (dissolved fraction) or triplicate measurements (<1000 kDa fraction and unfiltered samples) of one sample was lower than 5%. The blank, i.e. the background value of Fe in the MQ water and chemicals, is defined as the calculated amount of photons measured at 0 s loading time. Blank values varied slightly between the different days, but did not exceed 80 pM. The lowest detection limit, defined as three times the standard deviation of the blank (De Jong et al., 1998), was 11, 1 and 8 pM for the measurements of the unfiltered, dissolved and <1000 kDa fractions, respectively. SAFe reference water D2 was measured for validation of the system; we found 0.89 ± 0.01 nM ($n=2$) for SAFe D2. This corresponds well with the value of 0.91 ± 0.17 nM (Johnson et al., 2007).

2.3. Determination of iron speciation

The three size-fractions (unfiltered, <0.2 μm and <1000 kDa) were subjected to Fe titration and voltammetry on board. Unfiltered samples were kept in the dark at 4 °C and measured within 3 days to avoid any influence of biological activity. The two smaller size fractions were kept frozen if analysis could not be performed within 4 days.

2.3.1. Voltammetric procedure and sample treatment

Organic complexation of iron was determined by competing ligand exchange–adsorptive stripping voltammetry (CLE-AdSV) using 2-(2-thiazolylazo)-p-cresol (TAC) as a competing ligand (Croot and Johansson, 2000). The voltammetric equipment consisted of a μAutolab potentiostat (Type II, Ecochemie, The Netherlands), a mercury drop electrode (model VA 663 from Metrohm). The mercury drop size was approximately 0.25 mm^2. The reference electrode was double-junction, Ag/AgCl, 3 M KCl, with a salt bridge filled with 3 M KCl and a glassy carbon counter-electrode. Samples were stirred with a PTFE Teflon stirrer (3000 rpm). A current filter (Fortress 750, Best Power) to which the equipment was linked was used to prevent electrical noise.

Samples were pipetted into 13 Teflon bottles including 2 blanks (15 ml each). Seawater was buffered to pH 8.05 by adding a mixed NH_3/NH_4OH borate buffer. The buffer stock was 1 M boric acid (Suprapur, Merck) in 0.25 M ammonia (Suprapur, Merck) cleaned through a SepPak C18 column with 20 μM TAC. A stock of 0.02 M TAC was prepared in 3QD-methanol for a final concentration of 10 μM in seawater (Croot and Johansson, 2000). For the titrations a series of additions of Fe(III) standard from 0 to 8 nM was done in Teflon bottles with a stock of 10^{-6} M Fe(III) (prepared in 0.03 M HCl, Seastar chemicals Inc.). The titration series was left overnight to equilibrate before measurement. Before each titration series, the voltammetric Teflon cell was cleaned using blank solution. The chemical blank was below the detection limit of the method, being 0.027 nM $[Fe(TAC)_2]$ obtained by calculating three times the noise.

All Teflon vials were conditioned two times beforehand by preparing a titration with iron additions (0.33, 0.5, 0.67, 1, 1.5, 2, 2.5, 3, 4, 6, 8 nM).

Each equilibrated aliquot was transferred into the voltammetric Teflon cell and purged with nitrogen for 180 s. The differential pulse method was used. The deposition potential of −4 V was applied during 140–200 s and the sample was stirred to allow a better adsorption of the complex Fe–$(TAC)_2$ on the mercury drop. An equilibration time of 5 s without stirring was done before scanning between –0.4 and −0.7 V at 1.95 mV s^{-1} (modulation amplitude was 25.05 mV). Modulation time was 0.01 s and interval time was 0.1 s. The visible peak due to the dissociation of the Fe-complex was found between −0.460 and −0.500 V. Each measurement was done at least twice.

2.3.2. Calculation of iron speciation.

Ligand concentrations [Lt], conditional stability constants $\log K'$ and their respective standard deviations were calculated using the Langmuir model (Eq. (1), nonlinear regression of the Langmuir isotherm, Gledhill and van den Berg, 1994; Gerringa et al., 1995). By using the Langmuir model it is assumed that equilibrium between all Fe(III) species exists, all binding sites between Fe and the unknown ligand Lt are equal and binding is reversible. Eq. (1) assumes the existence of one organic ligand, and a one to one coordination:

$$[FeL] = \frac{K' \times [Fe^{3+}] \times [Lt]}{(1 + K' \times [Fe^{3+}])} \quad (1)$$

where [FeL] is the concentration of natural iron–ligand complexes, [Lt] the total ligand concentration and $[Fe^{3+}]$ the ionic iron concentration. [FeL] and $[Fe^{3+}]$ were calculated following the Eqs. (2) and (3), respectively.

$$[FeL] = [Fe_{fraction}] + [Fe_{added}] - [Fe(TAC)_2] \quad (2)$$

$[Fe_{fraction}]$ is the iron concentration measured by FIA in the unfiltered (Fe_{UNF}), the dissolved (DFe) and in the < 1000 kDa fractions ($Fe_{< 1000\ kDa}$). $[Fe_{added}]$ is the added iron from the titration:

$$\left[Fe^{3+}\right] = \frac{[Fe(TAC)_2]}{\alpha_{Fe(TAC)2}} \quad (3)$$

where $[Fe(TAC)_2]$ represents the concentration of the iron bound to TAC calculated by dividing the peak height (nA) by the slope (S=sensitivity) of the straight part of the titration curve. The sensitivity has been corrected for the influence of ligand sites not yet saturated, as explained by Turoczy and Sherwood (1997) and Hudson et al. (2003). The correction here was not done by an iterative procedure but by an algebraic solution of the equilibrium equations, in which S is determined together with Lt and K'. The estimated parameters are given with standard deviation of the fit of the data to the model:

$$\alpha_{Fe(TAC)2} = \beta_{Fe(TAC)2} \times [TAC]^2 = 10^{12.4}$$

with $\beta_{Fe(TAC)2}$ the conditional stability constant of iron with TAC assuming an equilibrium:

$$\beta_{Fe(TAC)2} = [Fe(TAC)_2]/[Fe^{3+}] \times [TAC]^2 = 10^{22.4}$$

with $[TAC] = 10^{-5}$ M (Croot and Johansson, 2000).

3. Results

Station 14 was located west of the coast of Portugal, north of the Strait of Gibraltar (Fig. 2). A surface mixed layer (SML) of about 50 m depth existed with relatively constant salinity (36.05) and decreasing potential temperature (15.3–14.8 °C, Fig. 3). Below the SML both the potential temperature and salinity decreased to a minimum of 11.5 °C and 35.7, respectively, at about 550 m depth. Below this depth, both salinity and potential temperature increased again, but to separate maxima around 1100 and 800 m depth, respectively, representing the lower and upper cores of the Mediterranean overflow water (MOW, Ambar et al., 2008; Fig. 3). The minimum of salinity and potential temperature at 550 m depth separated the MOW and the NACW (van Aken 2001). At about 2000 m depth the NADW proper was found and below 4000 m low deep water was recognised, with Antarctic bottom water (AABW) influence (for more details, see Measures et al., 1995; Laës et al., 2003).

The fluorescence (given by the CTD sensor in relative arbitrary units) showed maximum values of 0.8 at 38 m depth, and

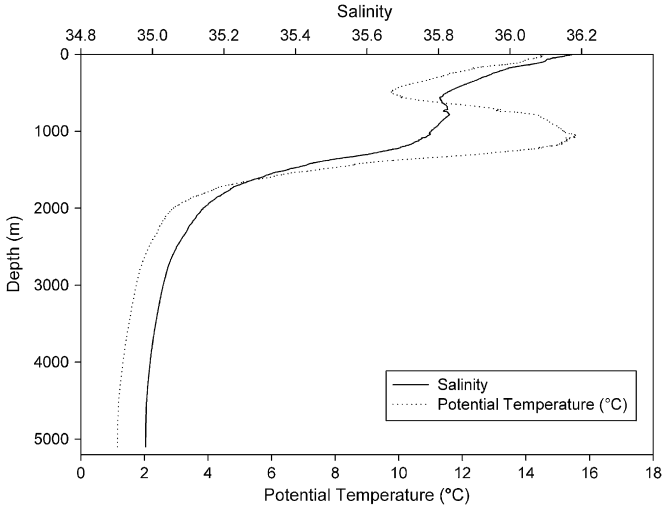

Fig. 3. Vertical profile of mean values of salinity and temperature from six hydrocasts at station 14 (1, 4, 7, 15, 18 and 20).

decreased to values <0.1 below 120 m depth (Fig. 4). The fluorescence provides an indication of the abundance of Chlorophyll *a*, i.e. the abundance of phytoplankton.

Iron was measured in three size fractions (Tables 1A, B, 2B, Fig. 5). The $Fe_{<1000\ kDa}$ concentrations (Table 1B) were very low; 0.02 nM in the SML increasing gradually to 0.22 nM at 2000 m and to 0.143 nM at 4000 m depth (bottom depth at station 14 was 5300 m). The concentrations of DFe showed a typical Fe profile shape, with very low values (0.1 nM) in the SML. The concentrations of DFe increased to a maximum of 0.69 nM at 500 m. Slightly lower concentrations were measured at mid-depth in the MOW (0.57 nM at 1000–2000 m depth) below which they increased again to concentrations of 0.65–0.7 nM at 3000–4000 m depth. Iron in the unfiltered (Fe_{UNF}) samples was measured at the lowest concentrations in the SML (0.95 nM). A broad maximum concentration was found in the MOW (4.1 nM). Below the MOW the concentrations decreased to values close to and lower than 2 nM.

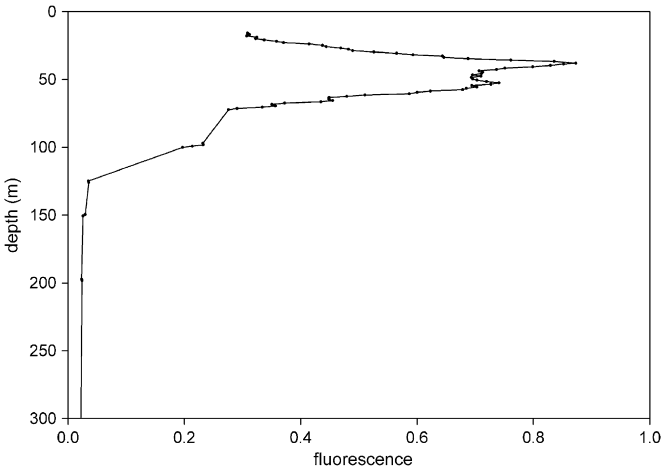

Fig. 4. Fluorescence (arbitrary units, a.u.) with depth (m) at station 14, cast 1.

A small maximum of 2.77 nM (one data point only) was also measured at 200 m depth.

The ligand characteristics are presented in Tables 1 and 2, where the total ligand concentration Lt is shown together with Excess L concentrations. The total ligand concentrations Lt more or less followed the Fe concentrations from the same fraction. Showing Excess L (Fig. 6) the data is made almost (see discussion) independent of the used Fe concentration. In this study this was relevant for two reasons: first because DFe concentration was measured, although at the same station, in samples from a different cast (18) than the cast (1) in which the speciation measurements were done; second because the measured Fe_{UNF} (dissolvable) was not necessarily the reversibly complexed Fe in those unfiltered samples. It is to be expected that not all Fe_{UNF} is bound reversibly to ligand and adsorption sites. However, it is unknown which percentage is irreversibly bound. For example inside mineral particles Fe is refractory (not dissolvable) at normal ocean pH conditions (pH$\sim$8) but may (partly) have dissolved during the 1 year acidification at the pH 1.8. In order to better understand the influence of an unknown concentration of Fe (not participating in reversible adsorption and ligand binding) on the results of the concentrations of ligand and Excess L and on K', the speciation data of the unfiltered fraction was calculated with the two extreme Fe concentrations, the minimum being the DFe concentration and the maximum being Fe_{UNF} concentrations (dissolvable).

The Excess L concentrations of the dissolved and <1000 kDa fractions were relatively high in the surface SML, 1.08 and 1.32 Eq of nM Fe, respectively (Tables 1 and 2 and Fig. 6). Below the SML Excess L concentrations in both fractions decreased steeply to 0.45 and 0.40 Eq of nM Fe, respectively. Excess L in the <1000 kDa fraction had a small maximum at 500 m depth (near 1 Eq of nM Fe). Both fractions (dissolved and <1000 kDa) showed an increase in Excess L concentrations from the MOW to 2000 m depth from 0.2 to 1 and 0.5 to 0.7 Eq of nM Fe, respectively, and remained more or less constant with depth below 2000 m. Excess L in the unfiltered samples have comparable concentrations for the calculations using two different Fe concentrations (DFe and Fe_{UNF}), thus proving that the Excess L concentration as such is

Table 1
Results of Fe and Fe speciation measurements for two size fractions: <0.2 μm (A) and <1000 kDa (B). [Excess L]=[Lt]−[Fe]. Alpha=K' × [Excess L].

A	Depth (m)	$[DFe]_{cast18}$ (nM)	SD	[Lt] (Eq of nM Fe)	SD*	log K' (mol^{-1})	SD*	[Excess L] (Eq of nM Fe)	log alpha	Excess L /DFe	*S*	SD*	R^{2*}
<0.2 μm	26	*0.130*	*0.002*	1.21	0.31	21.68	0.31	1.08	12.71	8.31	2.62	0.11	0.997
	102	*0.200*	*0.012*	0.65	0.19	21.93	0.31	0.45	12.58	2.25	2.00	0.07	0.997
	202	*0.460*	*0.046*	0.87	0.07	22.64	0.41	0.41	13.25	0.89	2.19	0.03	0.999
	501	*0.690*	*0.014*	1.00	0.08	22.71	0.37	0.31	13.20	0.45	2.09	0.04	0.998
	800	*0.670*	*0.005*	0.93	0.08	22.57	0.37	0.26	12.98	0.39	2.10	0.03	0.999
	999	*0.570*	*0.002*	0.80	0.08	23.00	0.36	0.23	13.36	0.40	1.31	0.03	0.998
	1998	*0.580*	*0.018*	1.59	0.26	21.83	0.23	1.01	12.83	1.74	2.18	0.09	0.997
	3497	*0.670*	**	1.76	0.13	22.11	0.13	1.09	13.15	1.63	2.46	0.07	0.998
	3998	*0.700*	*0.019*	1.54	0.06	22.91	0.29	0.84	13.83	1.20	1.14	0.02	0.999
B	**Depth (m)**	**$[Fe_{<1000\ kDa}]$ (nM)**	**SD**	**[Lt] (Eq of nM Fe)**	**SD***	**log K' (mol^{-1})**	**SD***	**[Excess L] (Eq of nM Fe)**	**log alpha**	**Excess L/$Fe_{<1000\ kDa}$**	***S***	**SD***	**R^{2*}**
<1000 kDa	26	0.029	0.008	1.35	0.18	22.02	0.25	1.32	13.14	45.52	1.06	0.03	0.998
	102	0.019	0.159	0.42	0.11	22.47	0.43	0.40	13.08	21.31	1.58	0.04	0.998
	202	0.047	0.083	0.51	0.12	22.32	0.34	0.46	12.99	9.68	2.16	0.05	0.998
	501	0.088	0.051	1.10	0.06	22.45	0.13	1.01	13.46	11.48	0.50	0.01	0.999
	800	0.077	0.083	0.61	0.12	21.98	0.40	0.53	12.71	6.83	2.28	0.05	0.997
	999	0.129	0.051	0.70	0.14	22.04	0.34	0.57	12.80	4.46	2.51	0.06	0.999
	1998	0.220	0.014	0.93	0.14	22.14	0.29	0.71	13.00	3.23	2.48	0.07	0.999
	3497	0.164	0.067	1.19	0.07	22.32	0.15	1.03	13.33	6.24	0.49	0.01	0.999
	3998	0.143	0.025	0.89	0.08	22.20	0.20	0.75	13.07	5.20	0.61	0.01	0.999

* Standard deviation and R^2 of the fit of the parameters Lt, K' and *S* using the nonlinear Langmuir model.
** Mean value of upper and lower concentrations: 0.64 and 0.7 nM at 3000 and 4000 m, respectively

Table 2
Results of Fe and Fe speciation measurements for the unfiltered samples. A shows the results of the speciation calculations using DFe concentrations (< 0.2 μm from cast 18). B shows the speciation results using the Fe_{UNF} concentrations. The parameters are the same as those presented in Table 1.

A	Depth (m)	$[DFe]_{cast18}$ (nM)	SD	[Lt] (Eq of nM Fe)	SD*	log K' (mol^{-1})	SD*	[Excess L] (Eq of nM Fe)	log alpha	Excess L/DFe	S	SD*	R^2*
	26	*0.130*	*0.002*	0.89	0.14	22.28	0.53	0.76	13.16	5.83	2.53	0.07	0.997
	102	*0.200*	*0.012*	1.27	0.07	22.71	0.24	1.07	13.74	5.37	1.06	0.02	0.994
	202	*0.460*	*0.046*	1.55	0.19	22.46	0.73	1.09	13.50	2.38	2.20	0.08	0.997
	501	*0.690*	*0.014*	2.12	0.57	21.55	0.21	1.43	12.70	2.07	2.33	0.21	0.997
	800	*0.670*	*0.005*	1.40	0.13	22.78	0.32	0.73	13.64	1.09	1.10	0.03	0.996
	999	*0.570*	*0.002*	1.10	0.08	22.27	0.15	0.53	13.00	0.94	4.13	0.08	0.999
	1998	*0.580*	*0.018*	1.75	0.10	22.70	0.31	1.17	13.76	2.01	0.61	0.01	0.997
	2998	*0.640*	*0.005*	2.00	0.24	21.75	0.14	1.36	12.88	2.12	2.37	0.08	0.998
	3497	*0.670*	**	1.29	0.07	22.85	0.40	0.62	13.64	0.92	1.21	0.02	0.998
	3998	*0.700*	*0.019*	1.51	0.08	23.07	0.54	0.81	13.97	1.15	1.10	0.03	0.997
B	**Depth (m)**	**$[Fe_{UNF}]$ (nM)**	**SD**	**[Lt] (Eq of nM Fe)**	**SD***	**log K' (mol^{-1})**	**SD***	**[Excess L] (Eq of nM Fe)**	**log alpha**	**Excess L /Fe_{UNF}**	***S***	**SD***	**R^2***
	26	0.953	0.016	1.74	0.12	22.52	0.28	0.79	13.42	0.82	2.54	0.07	0.997
	102	0.906	0.018	1.96	0.06	23.01	0.23	1.06	14.03	1.17	1.06	0.02	0.998
	202	2.767	0.049	3.89	0.16	22.82	0.31	1.12	13.87	0.41	2.21	0.08	0.994
	501	2.153	0.169	3.33	0.24	22.10	0.14	1.17	13.17	0.54	2.37	0.09	0.997
	800	3.788	0.069	4.50	0.11	23.40	0.71	0.71	14.26	0.19	1.09	0.03	0.996
	999	4.097	0.018	4.56	0.06	23.17	0.15	0.46	13.84	0.11	4.07	0.07	0.999
	1998	2.264	0.032	3.41	0.08	23.10	0.28	1.15	14.16	0.51	0.61	0.01	0.997
	2998	1.747	0.038	2.84	0.13	22.23	0.11	1.10	13.27	0.63	2.30	0.05	0.999
	3497	1.999	0.049	2.71	0.06	23.13	0.26	0.71	13.98	0.35	1.24	0.02	0.999
	3998	1.535	0.052	2.47	0.07	23.14	0.26	0.93	14.11	0.61	1.15	0.03	0.998

* Standard deviation and R^2 of the fit of the parameters Lt, K' and S using the nonlinear Langmuir model.
** Mean value of upper and lower concentrations: 0.64 and 0.7 nM at 3000 and 4000 m respectively

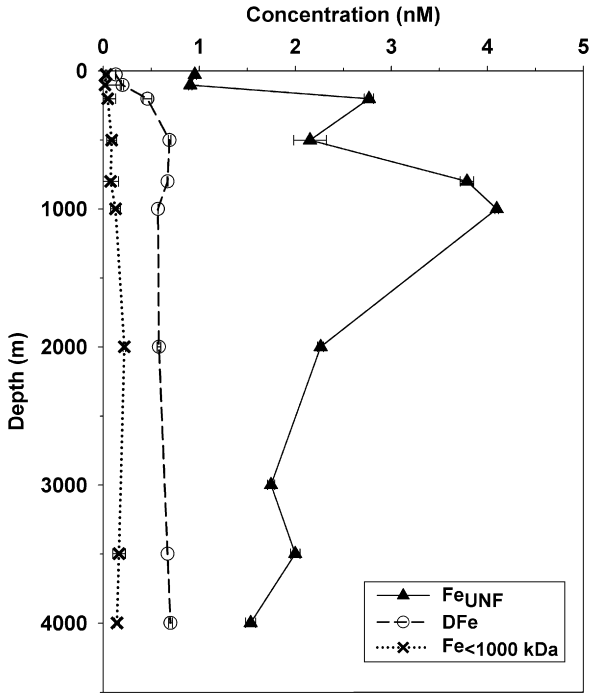

Fig. 5. Concentrations of Fe (in nM) with depth in the three size fractions: in unfiltered samples, < 0.2 μm and < 1000 kDa. Unfiltered and < 1000 kDa Fe concentrations are from cast 1, < 0.2 μm Fe concentrations are from cast 18. The standard deviation of the duplicate measurements (< 0.2 μm fraction) or triplicate measurements (< 1000 kDa and unfiltered fractions) is given.

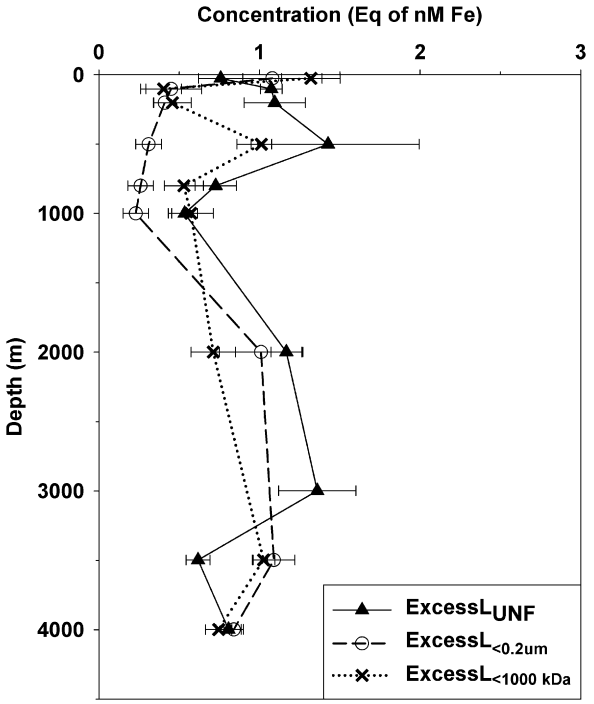

Fig. 6. Concentrations with depth of excess ligands ([Excess L]) in equivalents of nano-molar iron (Eq of nM Fe) in the three size fractions: unfiltered samples, < 0.2 μm and < 1000 kDa. The estimated parameters are given with standard deviation of the fit of the data to the model.

independent of the Fe concentration. Compared to the two smaller size fractions Excess L concentrations were larger in the layer between 100 and 2000 m. This layer comprised the MOW proper (800–1000 m), and MOW mixed with NACW above it and with NADW below it. In the deep waters of the NADW proper, Excess L concentrations in unfiltered samples were comparable to the other two smaller size fractions.

To determine the relation between the concentration of Excess L and Fe within the same fraction, the ratio of the two concentrations ([Excess L]/[Fe]) was used (Fig. 7, Tables 1 and 2).

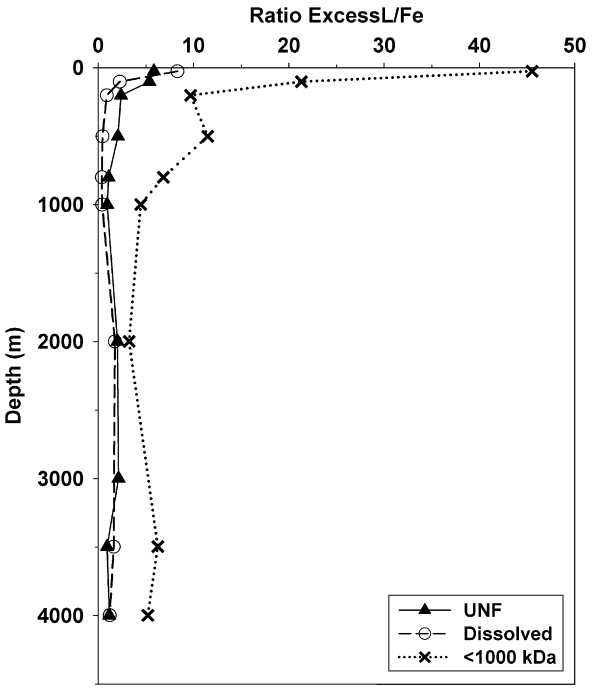

Fig. 7. The ratio of Excess L and Fe concentrations ([Excess L]/[Fe]) per size fraction with depth.

The Excess L over Fe was evident in the surface layer for all fractions (Thuróczy et al., in press). Relatively more Excess L sites were present in the smallest size fractions.

The conditional stability constant K' of the binding between the ligands and Fe was more or less equal for the two finer fractions, average values being $10^{22.38}$ and $10^{22.22}$ for dissolved and <1000 kDa, respectively (Tables 1A and B). The value of K' of the unfiltered samples was comparable when DFe concentrations were used (average $K'=10^{22.39}$) but higher (average $K'=10^{22.86}$) when the Fe_{UNF} concentrations were used (Tables 2A and B).

4. Discussion

4.1. Iron

The concentrations of DFe measured here were comparable to Fe profiles more to the south west of the Canary Islands reported by Sarthou et al. (2007), de Baar et al. (2008) and Rijkenberg et al. (2008a) in surface waters. The deep water concentration of DFe was also consistent with those reported by Ussher et al. (2007) on a transect in the Eastern North Atlantic Ocean (46°N, 8°W–52°N, 4°E), and values of DFe (<0.4 μm) in the upper 1000 m at a station (40°N, 20°W) reported by Measures et al. (2008). The mean concentration of 0.7 nM for DFe between 2000 and 4000 m depth in this study was very close to DFe (<0.4 μm) concentrations measured by Wu et al. (2001; 0.6–0.7 nM Fe) in the north Atlantic Ocean and Bergquist et al. (2007; 0.4–0.8 nM Fe) in the western North Atlantic Ocean.

Wu et al. (2001), Cullen et al. (2006) and Bergquist et al. (2007) also measured soluble Fe (their fraction was <0.02 μm). Below 2000 m depth we measured 0.13–0.22 nM Fe which was slightly lower than those found by Wu et al. (2001, 0.2–0.3 nM Fe), Bergquist et al. (2007, 0.2–0.4 nM Fe) and the deep data from Cullen et al. (2006, 0.22–0.28 nM Fe).

No distinction between MOW and the other water masses could be made in the concentrations of DFe. However, there was a strong signal in Fe concentrations of the unfiltered samples. Fe_{UNF} was much higher in the MOW than in the Atlantic water masses, which was not observed Sarthou et al. (2007) because of a different sampling strategy.

The position of the MOW in the water column did not make possible the interpretation of processes occurring as gradual trends with increasing depth, as discussed by Wu et al. (2001). Apparently the high Fe_{UNF} in the MOW was transported mainly laterally. Our station was located relatively far away from the Mediterranean outlet. The net horizontal velocity of lenses of MOW is of the order of a few cm/s (after Ambar et al., 2008), although the velocity within the whirls is much larger (up to 60 cm/s; Ambar et al., 2008). The MOW would have taken at least a few months if not more than a year to reach our sampling location. The vertical sinking velocity of diatoms is a relatively high (15–100 m per day for *Chaetoceros sp*. according to Passow, 1991 and van Haren et al., 1998). Within 50 days they would have sunk out of the MOW. Therefore, the particles containing Fe remaining in the MOW must be of a colloidal nature. It must be noted that the sparse sampling below the MOW did not permit further interpretation of these processes.

4.2. Fe-binding ligands

High concentrations of Fe-binding ligands in the surface layer have also been observed by Gerringa et al. (2006) in the Atlantic Ocean west of the Canary Islands and by Thuróczy et al. (in press) in the Atlantic sector of the Southern Ocean, who found high concentrations but also large variations in the dissolved organic ligand concentration above the chlorophyll maximum. A relation between phytoplankton characteristics and ligand concentrations existed within and below the chlorophyll maximum (Gerringa et al., 2006). In the present study, although the sampling was not directed towards small scale differences in the vertical upper layer of the ocean, the highest concentrations of ligands were found at 50 m depth in the dissolved and <1000 kDa fractions, indicating that phytoplankton could be the source of dissolved organic ligands, as observed by others (Rue and Bruland, 1997; Boye et al., 2001; Croot et al., 2001). In the upper 100 m, the K' values in the dissolved fraction of this research ($10^{20.9}$–$10^{21.7}$) fitted the range of those found by Gerringa et al. in the upper 150 m (2006; $10^{19.8}$–$10^{22.7}$) in the same fraction. Also Boye et al. (2003) found relatively low K' values in surface waters at 41°N ($10^{20.6}$–10^{21}). This indicated that the ligands presumably coming from the phytoplankton are relatively weak, supporting the conclusion of Rijkenberg et al. (2008b) that phytoplankton can modify ligand characteristics. Others stated that ligands related to phytoplankton activity belong to the relatively strong ligand group (Rue and Bruland, 1997; Cullen et al., 2006; Hunter and Boyd, 2007).

The results in Table 2 from the calculation of the ligand characteristics of unfiltered samples using two different Fe concentrations, DFe and Fe_{UNF}, illustrated that Excess L concentration was hardly influenced by the Fe concentration. This is valid as long as the titration data fits well to the model of Langmuir. Indeed, the discrepancies in Excess L concentrations at 500 and 3000 m depth for unfiltered sample were caused by a relatively bad fit of the model. By adding Fe_{UNF} to the Excess L concentration, the upper limit of the total ligand concentration was obtained (Table 2B), whereas the lower limit was obtained by the addition of the DFe (Table 2A). However, the K' values were quite different between the two calculations (Table 2). Consequently, a 2.2–7.3 times higher [$Fe_{fraction}$] (Eq. (2)) resulted in a 1.24–7.16 higher K' value leading to a difference in log K' of 0.09–0.85. Therefore the calculation of K' is sensitive to refractive Fe that is irreversibly bound in colloids or particles and can be

artificially increased by a too high [$Fe_{fraction}$]. Part of Fe bound in the high molecular weight fraction (between 1000 kDa and 0.2 μm) may be not exchangeable, as already suggested by Cullen et al. (2006). Hitherto it was assumed that all Fe in the samples was reversibly bound by ligands. This assumption has consequences on parameters as the alpha factor which would be overestimated. Alpha (Tables 1 and 2), the product of K' and the Excess L, represents the reactivity of the ligands and reflects the equilibrium between Fe and ligands. A high alpha favours Fe solubilisation via organic complexation (large Excess L, or strong ligands, or both). Reversely, a low alpha favours Fe loss from solution via precipitation and or scavenging.

4.3. Complexation versus scavenging in the water column

Wu et al. (2001) showed that soluble Fe (defined as <10 kDa) and soluble ligands were depleted in surface waters, then increased to a maximum at 100 m depth, after which they both decreased most likely due to colloid aggregation and scavenging of Fe. They concluded that a competition exists between empty soluble ligand sites and adsorption sites on colloids and particles, and that colloid aggregation may cause a net export of Fe from the water column to the sediments (Fig. 1). Although we do not have the smallest size fraction of the truly soluble (<10 kDa), the two dissolved size fractions and the unfiltered samples allow us to see trends due to colloid aggregation or solubilisation with depth. The ratio of Excess L over Fe ([Excess L]/[Fe]) per size fraction indicates a relative competitive force (Thuróczy et al., in press, using [Lt]/[Fe]) since it reflects the relative saturation of the natural ligands with Fe. A ratio near 0 means saturation of the Excess L that can lead to Fe precipitation if Fe is dissolved and scavenging if Fe is in the particulate fraction (>0.2 μm). Reversely, high ratios in the dissolved fractions mean Fe depletion and a high potential for Fe solubilisation. For the two smaller size fractions (<0.2 μm and <1000 kDa, Fig. 7, Table 1), [Excess L]/[Fe] was high in the surface followed by a steep decrease to reach low and more or less constant values with depth. Surface ratios of 11 and 45 decreased to 2–0.4 and 3–10 (for <0.2 μm and <1000 kDa, respectively); thus a high potential for binding Fe inputs (by rain, dust or remineralisation) existed. Ligands were unsaturated because of Fe uptake by phytoplankton.

According to Bergquist et al. (2007), the variability of DFe with depth is due to the variability of the colloidal Fe (between 0.02 and 0.4 μm; here colloidal Fe is assumed to be between 1000 kDa and 0.2 μm), illustrated by the linear relationship [$Fe_{<0.4\,\mu m}$]=1.18 [$Fe_{0.02-0.4\,\mu m}$]+0.29 ($R^2=0.85$). A slope of 1.18 being near 1 showed that the changes in concentrations were attributed to the colloidal Fe pool, and that the soluble Fe concentration remained 0.29 nM. We also found a similar relationship: [$Fe_{<0.2\,\mu m}$]=1.16 [$Fe_{1000\,kDa-0.2\,\mu m}$]+0.03 ($R^2=0.93$, $n=9$). The slopes were identical; however, the y-cut-off was ten times lower, nearly zero. Therefore we can conclude that colloidal Fe determines the changes in dissolved concentration, but then soluble Fe (here <1000 kDa) does not a play any role.

Since the ligands are assumed to be organic, the presence of phytoplankton and co-existing organisms like bacteria is one of the possible sources (Rue and Bruland, 1997; Butler, 1998, 2005; Boye and van den Berg, 2000; Croot et al., 2001; Barbeau et al., 2001; Maldonado et al., 2005; Gerringa et al., 2006). The trend of the [Excess L]/[Fe] with depth was the same for the different fractions, but the absolute values heavily depend on the Fe concentration used in the calculation for the unfiltered sample (Table 2A and B). The ratio of Excess L between the fractions <0.2 μm and <1000 kDa (Fig. 8) was near 1 in the whole water column. It was even slightly below 1 in samples from the upper 1000 m, which is in theory not possible, as empty sites present in the smaller fraction should also be present in the total sample. Filtration might cause a disequilibrium in the samples, in which the smallest and most reactive fraction (Nishioka et al., 2001, 2005; Cullen et al., 2006) exchanges Fe during filtration. Thus empty ligand sites occur predominantly in the fraction <1000 kDa. The disequilibrium might be caused by colloidal formation as suggested by Kondo et al. (2008). Contamination is to be excluded since [$Fe_{<0.2\,\mu m}$] is always larger than [$Fe_{<1000\,kDa}$].

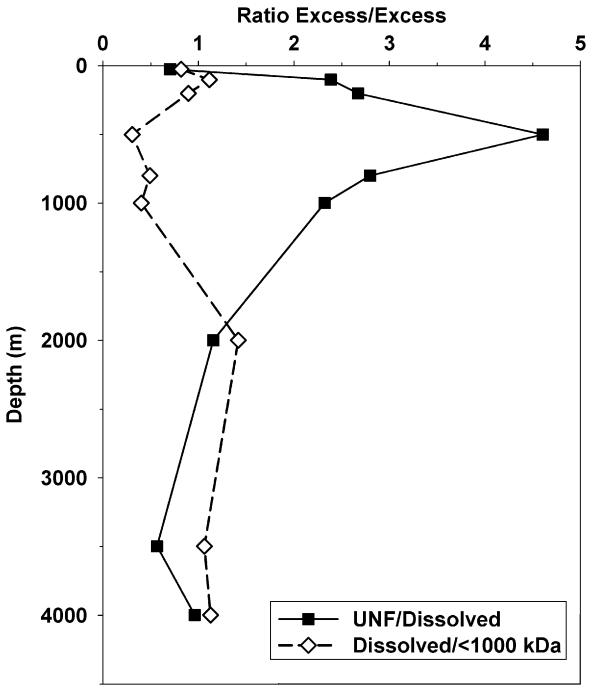

Fig. 8. Ratios [Excess L_{UNF}]/[Excess $L_{<0.2\,\mu m}$] and [Excess $L_{<0.2\,\mu m}$]/[Excess $L_{<1000\,kDa}$] with depth.

According to the temperature/salinity diagram presented by Middag et al. (submitted for publication), the NADW started at 1750–2000 m, which was also the boundary for the changes in iron parameters such as Fe_{UNF} and the ratio of Excess L between the fractions [Excess L_{UNF}]/[Excess $L_{<0.2\,\mu m}$] and [Excess $L_{<0.2\,\mu m}$]/[Excess $L_{<1000\,kDa}$] (Figs. 5 and 8). The ratio of Excess L between the fractions [Excess L_{UNF}]/[Excess $L_{<0.2\,\mu m}$] and [Excess $L_{<0.2\,\mu m}$]/[Excess $L_{<1000\,kDa}$] informs us which size fraction has the highest potential to bind Fe. Theoretically these ratios should be equal or higher than 1. When the ratio is larger than one, the larger fraction has more empty ligand sites (i.e. Excess L) which are not present in the smaller fraction and has a potential to bind Fe. Between 50 and 2000 m (comprising the NACW and the MOW) a significant amount of Excess L existed in the unfiltered water (Fig. 8) and thus pointed to processes of reversible adsorption (complexation in the dissolved fraction). This was especially the case in the NACW, and to a lesser extent in the MOW (but the ratio was still 2). Thus the potential for scavenging was larger than for solubilisation between 50 and 2000 m.

High scavenging potential above the MOW can be explained by a previous dust deposition but also by sinking phytoplankton. Although the station was not located in the centre of the Sahara dust plumes (Bowie et al., 2002; Croot et al., 2004), Middag et al. (submitted for publication) detected the influence of dust input on dissolved Al, Mn and Fe concentrations. According to Bergquist and Boyle (2006) the residence time of Fe_{UNF} due to dust input is 1–5 months, thus dust input could explain the high concentrations of Fe_{UNF}. A contribution of sinking phytoplankton may partly explain the Fe_{UNF} maximum at a depth of 200 m. Mixing with

more Fe-saturated particles (ratio 2–2.5 compared to 4, Fig. 8) coupled with remineralisation might have resulted in solubilisation of Fe, explaining the small maximum in DFe at 500 m depth.

Scavenging only occurs if the adsorption sites on colloids or larger particles bind stronger than the dissolved organic ligands. This control can be expressed by the alpha factor of the organic ligands. Below 800 m depth, alpha of the ligands in the <1000 kDa fraction was remarkably constant at 10^{13} (Table 1). These ligands were unsaturated in the whole water column (Fig. 7) and thus 10^{13} as alpha factor seems to be an equilibrium value controlling scavenging and precipitation of Fe below 800–1000 m depth (Fig. 8). Colloid aggregation can occur in the fraction between 1000 kDa and 0.2 μm which was saturated with Fe over the whole water column.

Together with the conclusion from Wu et al. (2001), that Fe uptake by phytoplankton is preferably done from the soluble fraction, that part of the colloidal fraction is inert, and that the same organic ligands are present in both fractions, we come to a different conclusion than Bergquist et al. (2007) who suggested that the colloidal fraction is the one that changes, whereas the soluble one does not. The saturation of the ligands in both size fractions regulates the formation of inorganic Fe-colloids and particles, in which Fe is irreversibly bound. From our research we show that the ligands in the colloidal fraction were saturated, whereas in the whole water column the ligands in the soluble fraction were not saturated (here <1000 kDa). Thus the Excess L in the soluble fraction regulates dissolution and colloid aggregation with a remarkably stable alpha factor of 10^{13}. Is thus the solubility product or better the colloid aggregation product of Fe 10^{13}?

5. Conclusions

The concentrations of DFe and $Fe_{<1000\,kDa}$ followed a nutrient-type profile with depth: depleted at the surface by phytoplankton uptake, a modest increase until 500–1000 m, and more or less constant concentrations below. The Excess L concentrations of the dissolved and <1000 kDa fractions were relatively high in the SML, 1.08 and 1.32 Eq of nM Fe respectively. These high Excess L concentrations can be explained by Fe uptake increasing the empty ligand sites but also by ligand production by phytoplankton and bacteria.

The MOW was recognised by Fe_{UNF} concentrations twice higher than in the overlying and underlying Atlantic Water masses. Here the ligands were not completely saturated, thus equilibrium between adsorption and complexation existed.

Excess L proved to be a very useful parameter since it is independent of the Fe concentration, which is not the case for total ligand concentration, alpha factor and conditional stability constant. Excess L gives information on the binding potential of the ligands, especially when expressed in the ratio Excess L/Fe which reflects the relative saturation of the ligands.

The smallest size fraction which was less saturated with Fe had relatively more Excess L (<1000 kDa fraction $\gg$ dissolved fraction $\gg$ unfiltered sample), and consequently had the largest capacity to bind more Fe, confirming that this is the most reactive fraction. The ratio Excess L_{UNF}/Excess $L_{<0.2\,\mu m}$ being larger than 1 clearly showed that above 1000–2000 m unsaturated ligands existed in the unfiltered fraction, suggesting the removal of Fe from the dissolved phase by processes of reversible adsorption, whereas below 2000 m depth precipitation would be the major process of Fe removal. In the whole water column, the organic ligands in the larger colloidal fraction (between 1000 kDa and 0.2 μm) were saturated with Fe. The controlling alpha factor of the ligands ($[\text{Excess L}]\times K'$) of the <1000 kDa fraction was relatively constant at 10^{13} in the NADW and in the MOW, and might reflect the equilibrium between dissolved and particulate in these water masses.

Acknowledgements

We are most grateful to captain John Ellen and crew of R.V. Pelagia. We thank Jan van Ooyen (NIOZ) for the nutrients data and Marie Le Guitton for her review.

Jun Nishioka (Hokkaido University, Japan) was so kind to let us benefit from his knowledge of size fractionation. Jun Nishioka helped us further in obtaining the hollow fibre filters from Mitsubishi Rayon ltd.

This research is funded by NWO. Geotraces sub-project: 851.40.102.

References

Ambar, I., Serra, N., Neves, F., Ferraira, T., 2008. Observations of the Mediterranean undercurrent and eddies in the Gulf of Cadiz during 2001. J. Mar. Syst. 71 (1–2), 195–220.

Barbeau, K., Rue, E.L., Bruland, K.W., Butler, A., 2001. Photochemical cycling of iron in the surface ocean mediated by microbial iron(III)-binding ligands. Nature 413 (6854), 409–413.

Bergquist, B.A., Boyle, E.A., 2006. Dissolved iron in the tropical and subtropical Atlantic Ocean. Global Biogeochem. Cycles 20 (1), GB1015.

Bergquist, B.A., Wu, J., Boyle, E.A., 2007. Variability in oceanic dissolved iron is dominated by the colloidal fraction. Geochim. Cosmochim. Acta 71 (12), 2960–2974.

Boye, M., van den Berg, C.M.G., 2000. Iron availability and the release of iron-complexing ligands by *Emiliania huxleyi*. Mar. Chem. 70 (4), 277–287.

Boye, M., van den Berg, C.M.G., de Jong, J.T.M., Leach, H., Croot, P., de Baar, H.J.W., 2001. Organic complexation of iron in the Southern Ocean. Deep-Sea Res. I 48 (6), 1477–1497.

Boye, M., Aldrich, A.P., van den Berg, C.M.G., de Jong, J.T.M., Veldhuis, M., de Baar, H.J.W., 2003. Horizontal gradient of the chemical speciation of iron in surface waters of the northeast Atlantic Ocean. Mar. Chem. 80 (2–3), 129–143.

Boye, M., Nishioka, J., Croot, P.L., Laan, P., Timmermans, K.R., de Baar, H.J.W., 2005. Major deviations of iron complexation during 22 days of a mesoscale iron enrichment in the open Southern Ocean. Mar. Chem. 96 (3–4), 257–271.

Bowie, A.R., Whitworth, D.J., Achterberg, P., Mantoura, R.F.C., Worsfold, P.J., 2002. Biogeochemistry of Fe and other trace elements (Al, Co, Ni) in the upper Atlantic Ocean. Deep-Sea Res. I 49 (4), 605–636.

Butler, A., 1998. Acquisition and utilization of transition metal ions by marine organisms. Science 281 (5374), 207–210.

Butler, A., 2005. Marine siderophores and microbial iron mobilization. BioMetals 18 (4), 369–374.

Croot, P.L., Johansson, M., 2000. Determination of iron speciation by cathodic stripping voltammetry in seawater using the competing ligand 2-(2-Thiazolylazo)-p-cresol (TAC). Electroanalysis 12 (8), 565–576.

Croot, P.L., Bowie, A.R., Frew, R.D., Maldonado, M.T., Hall, J.A., Safi, K.A., La Roche, J., Boyd, P.W., Law, C.S., 2001. Retention of dissolved iron and Fe-II in an iron induced Southern Ocean phytoplankton bloom. Geophys. Res. Lett. 28 (18), 3425–3428.

Croot, P.L., Streu, P., Baker, A.R., 2004. Short residence time for iron in the surface seawater impacted by atmospheric dry deposition from Saharan dust events. Geophys. Res. Lett. 31 (23)L23S08.

Cullen, J.T., Bergquist, B.A., Moffett, J.W., 2006. Thermodynamic characterization of partitioning of iron between soluble and colloidal species in the Atlantic Ocean. Mar. Chem. 98 (2–4), 295–303.

De Baar, H.J.W., de Jong, J.T.M., 2001. Distributions, sources and sinks of iron in seawater. In: Turner, D.R., Hunter, K.A. (Eds.), The Biogeochemistry of Iron in Seawater. Wiley and sons Chapter 5, Fig. 5, pp. 135.

De Baar, H.J.W., Timmermans, K.R., Laan, P., de Porto, H.H., Ober, S., Blom, J.J., Bakker, M.C., Schilling, J., Sarthou, G., Smit, M.G., Klunder, M., 2008. Titan: a new facility for ultraclean sampling of trace elements and isotopes in the deep oceans in the international Geotraces program. Mar. Chem. 111 (1–2), 4–21.

De Jong, J.T.M., den Das, J., Bathmann, U., Stoll, M.H.C., Kattner, G., Nolting, R.F., de Baar, H.J.W., 1998. Dissolved iron at subnanomolar levels in the Southern Ocean as determined by ship-board analysis. Anal. Chim. Acta 377 (2–3), 113–124.

GEOTRACES Planning Group, 2006. GEOTRACES Science Plan, Scientific Committee on Oceanic Research, Baltimore, Maryland.

Gerringa, L.J.A., Herman, P.M.J., Poortvliet, T.C.W., 1995. Comparison of the linear van den Berg/Ružić transformation and a non-linear fit of the Langmuir isotherm applied to Cu speciation data in the estuarine environment. Mar. Chem. 48 (2), 131–142.

Gerringa, L.J.A., Veldhuis, M.J.W., Timmermans, K.R., Sarthou, G., de Baar, H.J.W., 2006. Co-variance of dissolved Fe-binding ligands with phytoplankton characteristics in the Canary Basin. Mar. Chem. 102 (3–4), 276–290.

Gledhill, M., van den Berg, C.M.G., 1994. Determination of complexation of iron (III) with natural organic complexing ligands in sea water using cathodic stripping voltammetry. Mar. Chem. 47 (1), 41–54.
Hudson, R.J.M., Rue, R.L., Bruland, K.W., 2003. Modeling complexometric titrations of natural water samples. Environ. Sci. Technol. 37 (8), 1553–1562.
Hunter, K.A., Boyd, P.W., 2007. Iron binding ligands and their role in the ocean biogeochemistry of iron. Environ. Chem. 4 (4), 221–232.
Johnson, K.S., Boyle, E., Bruland, K., Measures, C., Moffett, J., Aquilarislas, A., Barbeau, K., Cai, Y., Chase, Z., Cullen, J., Doi, T., Elrod, V., Fitzwater, S., Gordon, M., King, A., Laan, P., Laglera-Baquer, L., Landing, W., Lohan, M., Mendez, J., Milne, A., Obata, H., Ossiander, L., Plant, J., Sarthou, G., Sedwick, P., Smith, G.J., Sohst, B., Tanner, S., van den Berg, S., Wu, J., 2007. Developing standards for dissolved iron in seawater. Eos Trans. Am. Geophys. Union 88 (11), 131–132.
Kondo, Y., Takeda, S., Nishioka, J., Obata, H., Furuya, K., Johnson, W.K., Wong, C.S., 2008. Organic iron (III) complexing ligands during an iron enrichment experiment in the western subarctic North Pacific. Geophys. Res. Lett. 35 (12), L12601.
Klunder, M.B., Middag, R., de Baar, H.J.W., Laan, P. Dissolved Fe in the Southern Ocean (Atlantic sector). Deep-Sea Res. II, in press.
Kuma, K., Nishioka, J., Matsunaga, K., 1996. Controls on iron(III) hyrdroxide solubility in seawater; the influence of pH and natural organic chelators. Limnol. Oceanogr. 41 (3), 396–407.
Laës, A., Blain, S., Laan, P., Achterberg, E.P., Sarthou, G., de Baar, H.J.W., 2003. Deep dissolved iron profiles in the eastern North Atlantic in relation to water masses. Geophys. Res. Lett. 30 (17), 1902.
Lohan, M.C., Aguilar-Islas, A., Franks, R.P., Bruland, K.W., 2005. Determination of iron and copper in seawater at pH 1.7 with a new commercially available chelating resin, NTA superflow. Anal. Chim. Acta 530 (1), 121–129.
Maldonado, M.T., Strzepek, R.F., Sander, S., Boyd, P.W., 2005. Acquisition of iron bound to strong organic complexes, with different Fe-binding groups and photochemical reactivities, by plankton communities in Fe-limited subantarctic waters. Global Biogeochem. Cycles 19 (4), GB4S23.
Measures, C.I., Yeats, P.A., Schmidt, D, 1995. The hydrographic setting of the IOC base-line cruise to the eastern Atlantic 30-degrees-S to 35-degrees-N. Mar. Chem. 49 (4), 243–252.
Measures, C.I., Landing, W.M., Brown, M.T., Buck, C.S., 2008. High-resolution Al and Fe data from the Atlantic Ocean CLIVAR-CO2 repeat hydrography A16N transect: extensive linkages between atmospheric dust and upper ocean geochemistry. Global Biogeochem. Cycles 22 (1), GB1005.
Middag, R., De Baar, H.J.W., Laan, P., Bakker, K., 2009. Dissolved aluminium and the silicon cycle in the Arctic Ocean. Mar. Chem. 115 (3–4), 176–195.
Middag, R., Klunder, M.B., Thuróczy, C.E., Gerringa, L.J.A., de Baar, H.J.W., Timmermans, K.R., Laan, P. Aluminium, iron and manganese in relation to the silicon cycle in the Eastern North Atlantic Ocean. Deep-Sea Res. I, submitted for publication.
Millero, F.J., 1998. Solubility of Fe(III) in seawater. Earth Planet. Sci. Lett. 154 (1–4), 323–329.
Nishioka, J., Takeda, S., 2000. Change in the concentrations of iron in different size fractions during growth of the oceanic diatom *Chaetoceros sp.*: importance of small colloidal iron. Mar. Biol. 137 (2), 231–238.
Nishioka, J., Takeda, S., Wong, C.S., Johnson, W.K., 2001. Sized-fractionated iron concentrations in the northeast Pacific Ocean: distribution of soluble and small colloidal iron. Mar. Chem. 74 (2–3), 157–179.
Nishioka, J., Takeda, S., de Baar, H.J.W., Croot, P.L., Boye, M., Laan, P., Timmermans, K.R., 2005. Changes in the concentration of iron in different size fractions during an iron enrichment experiment in the open Southern Ocean. Mar. Chem. 95 (1–2), 51–63.
Passow, U., 1991. Species-specific sedimentation and sinking velocities of diatoms. Mar. Biol. 108 (3), 449–455.
Rue, E.L., Bruland, K.W., 1997. The role of organic complexation on ambient iron chemistry in the equatorial Pacific Ocean and the response of a mesoscale iron addition experiment. Limnol. Oceanogr. 42 (5), 901–910.
Rijkenberg, M.J.A., Powell, C.F., Dall'Osto, M., Nielsdottir, M.C., Patey, M.D., Hill, P.G., Baker, A.R., Jickels, T.D., Harrison, R.M., Achterberg, E.P., 2008a. Changes in iron speciation following a Saharan dust event in the tropical North Atlantic Ocean. Mar. Chem. 110 (1–2), 56–67.
Rijkenberg, M.J.A., Gerringa, L.J.A., Timmermans, K.R., Fischer, A.C., Kroon, K.J., Buma, A.G.J., Wolterbeek, H.Th., de Baar, H.J.W., 2008b. Enhancement of reactive iron pool by marine diatoms. Mar. Chem. 109 (1–2), 29–44.
Sarthou, G., Baker, A.R., Kramer, J., Laan, P., Laës, A., Ussher, S., Achterberg, E.P., de Baar, H.J.W., Timmermans, K.R., Blain, S., 2007. Influence of atmospheric inputs on the iron distribution in the subtropical North–East Atlantic Ocean. Mar. Chem. 104 (3-4), 186–202.
Thuróczy, C.-E., Gerringa, L.J.A., Klunder, M.B., Laan, P., de Baar, H.J.W. Observation of consistent trends in the organic complexation of dissolved iron in the Atlantic sector of the Southern Ocean. Deep-Sea Res. II, in press.
Turoczy, N.J., Sherwood, J.E., 1997. Modification of the van den Berg/Ruzic method for the investigation of complexation parameters of natural waters. Anal. Chim. Acta 354 (1–3), 15–21.
Ussher, S.J., Worsfold, P.J., Achterberg, E.P., Laës, A., Blain, S., Laan, P., de Baar, H.J.W., 2007. Distribution and redox speciation of dissolved iron on the European continental margin. Limnol. Oceanogr. 52 (6), 2530–2539.
van Aken, H.M., 2001. The hydrography of the mid-latitude Northeast Atlantic Ocean—Part III: the subducted thermocline water mass. Deep-Sea Res. I 48 (1), 237–267.
van Haren, H., Mills, D.K., Wetsteyn, L.P.M.J., 1998. Detailed observations of the phytoplankton spring bloom in the stratifying central North Sea. J. Mar. Res. 56 (3), 655–680.
Wu, J., Boyle, E., Sunda, W., Wen, L.-S., 2001. Soluble and colloidal iron in the oligotrophic North Atlantic and North Pacific. Science 293 (5531), 847–849.